Reviewer 2 Report Rebuttal

Please find a point by point response to the referee's comments. N.B. the referee's comments are in blue and our responses are in black. We also upload a copy of the manuscript in which changes from the previous version are highlighted for the referee's convenience.

Reviewer 2

This manuscript presents an experimental study of blade strain measurements on a wind turbine rotor using Rayleigh backscattering sensing (RBS). The authors investigate how gravity- and rotation-induced loads combine with aerodynamic loading, and propose a decomposition method to isolate centrifugal, gravitational, and aerodynamic strain contributions. Strain statistics are compared under quiescent background conditions and under controlled free-stream turbulence across a range of tip-speed ratios.

Overall, the manuscript is clearly written and the introduction provides a helpful overview of existing work and the remaining challenges in understanding the aerodynamics of rotating wind turbine blades. The experimental setup is impressive, and I believe the dataset itself could be valuable to the community. However, several key elements required to support the main conclusions are currently missing. In particular, the manuscript lacks adequate uncertainty quantification and sensor characterization, and a number of the subsequent data-processing assumptions appear insufficiently justified. As a result, some of the interpretations may not be supported by the presented evidence. I therefore recommend major revisions before the manuscript can be considered for publication in *Wind Energy Science* journal.

We appreciate the reviewer's thorough evaluation of our manuscript and valuable comments. We hope that the referee's concerns have been addressed in our revised manuscript.

Note to the reviewer:

The reviewers' comments prompted us to undertake a thorough, "root-and-branch" reappraisal of the manuscript as a whole. Beyond the specific points raised, this process led us to identify a number of areas where the scientific content, clarity, and rigour of the paper could be improved. We have therefore introduced several additional modifications that were not explicitly requested but which we believe significantly raise the scientific quality of the manuscript.

We have added section 2.4., clearly detailing the experimental protocol followed, specifying the two independent tests conducted to produce the datasets presented. Section 3 has been reshaped completely. We have added section 3.2. to include data from the blade's response to a static unidirectional load case, where we have explored the effect of incremental loads on the blade, to assess how it reacted under 3 different loading cases. Section 3.3. refers to the blade loads under a quiescent background, and we have now added the spectra of the strain under 3 representative rotation conditions under these circumstances. The spectra of the strain under quiescent conditions are presented in figure 9, which also provides key evidence for the aerodynamic origin of the $St_\Omega = 3$ signature in the blade strain spectra. We have updated the notation for the decomposed strain components throughout the revised manuscript: what was previously referred to as *flapwise strain* (ε^f) is now denoted *spanwise strain* (ε^s), and *edgewise strain* (ε^e) is now referred to as *chordwise strain* (ε^c). This change more accurately reflects the geometry of the fibre-optic sensor layout, which is aligned with the blade's spanwise and chordwise axes in the blade coordinate system $s\mathcal{O}c$, rather than with the classical structural flapwise/edgewise decomposition. The flapwise and edgewise bending moments (M^f and M^e) are retained where they refer to structural mechanics. Section 7 was also added to exploit the concurrent measurements we conducted in $T1$,

where we present cross-power spectral densities for representative test cases. We have also added the spanwise distributions of RMS(ε'_a) to figure 16 *a)* to complement the analogous distributions of time-averaged strain in figure 13. We have also added substantial material to the appendix for the benefit of clarity: appendix A details the homogeneity of the FST operating conditions across the span of the turbine; appendix B provides a detailed overview of uncertainty on the conducted hot-wire measurements, appendix C details the blade geometry used and aerofoil profiles chosen. Appendix D details the least-square detrending procedure used to correct strain signal drift observed in $T1$. The chordwise time-averaged strain have been moved to appendix E, reported for completeness and transparency rather than as a well-characterised aerodynamic finding.

Major comments:

1. Figure 1: How homogeneous is the free-stream turbulence (FST) across the test section and across the rotor disc? Is the FST characterization reported in a separate publication? If so, this should be cited explicitly. Otherwise, additional details (mean velocity profile, turbulence intensity distribution, integral length scales, and spatial uniformity) should be provided, either in the main text or in an appendix.

   The spatial homogeneity of the free-stream turbulence across the rotor disc was assessed through preliminary hot-wire measurements at multiple spanwise positions across the rotor's span. As shown in Figure A1 (Appendix "FST characterisation"), the profiles exhibit good spatial uniformity across the rotor span for the three FST "flavours".

   The variation of the normalized mean velocity profiles ($\overline{U}/U_\infty$) remain within $\pm 5\%$ across the span for all cases. The turbulence intensity (TI) profiles show a maximum variation of $\pm 7\%$ from the mean TI for each FST "flavour". The integral length scale profiles ($\mathcal{L}_{11}/R$) show the largest increased spatial variability, especially for FST "flavour" A and B.

   These profiles confirm that the FST conditions are sufficiently homogeneous across the rotor disc for the present experimental investigation. These profiles and discussion have been added to Appendix "FST characterisation", which we believe adequately addresses your concerns.

2. Section 2.2: The uncertainty of the RBS strain measurements is not quantified. The measured strain can depend on several factors, including the bonding/gluing procedure, sensor placement, temperature effects, and surface curvature. In addition, since the study relies on time-resolved data, the dynamic response and bandwidth of the sensing chain should be documented (or cited from prior validation studies). Finally, potential asymmetry in sensor response under tensile versus compressive loading should be addressed.

   We have quantified the uncertainty of the RBS in our previous work - see [1]. The bonding procedure followed the same procedure as described in [4, 1, 2]. A preliminary experiment to validate the RBS measurements was conducted, using a cantilevered cylinder and a weight (1.024 Kg) placed at its free-end. RBS and Strain gauges were used and aligned with the cylinder's spanwise extent. Figure 1 of the rebuttal presents the spatial strain results obtained with this experiment, and is a reproduction of the figure in the appendix of [1].

   The data was recorded simultaneously, and shows good spatial agreement, overestimating the strain gauge data by less than $5.5\mu\varepsilon$. To note that this might be driven by the fact that the sensors do not strictly share the same position across the cylinder to avoid overlapping. We have added a note on this and some more information on the acquisition system to the last paragraph of section 2.2 "Rayleigh backscattering sensors (RBS) strain measurements".

   Fibre-optic strain sensing can exhibit reduced sensitivity under compressive loading; however, this is mitigated here through pre-straining during bonding following [4, 1, 2]. We have added this information in the revised version of the manuscript - second paragraph of section 2.2. "Rayleigh backscattering sensors (RBS) strain measurements". A baseline is taken before acquisition, and the added-effects of compressive-load strain, which would result in a smaller tension across the fibre are then retrieved. Temperature effects can be neglected as the temperature was fixed using the 200 kW heat-exchanger of the tunnel, with variations of temperature during operation no larger than 0.3° C.

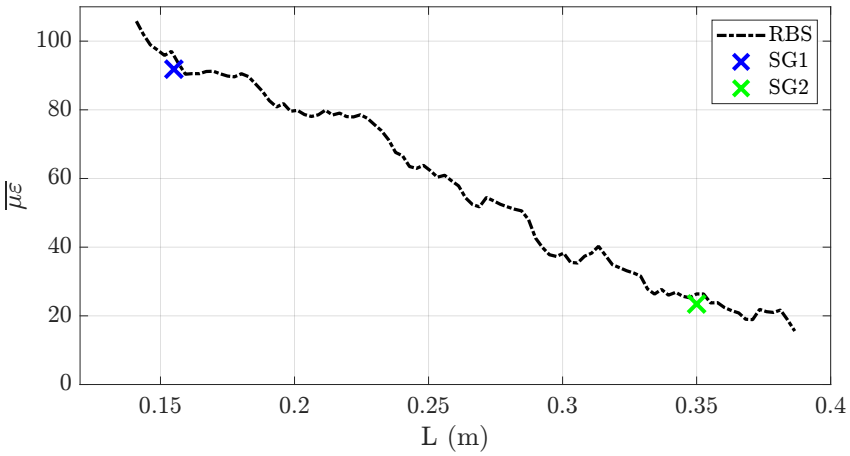

Figure 1: Preliminary experiment for RBS validation, comparing with two strain gauges (SG1 and SG2). For more details see [1].

The RBS interrogator operates at a sampling frequency of 100 Hz, providing sufficient bandwidth to resolve the aerodynamic forcing frequencies of interest (up to 45 Hz, well above the blade-passing frequency and its harmonics). Details of the fibre optic's dynamic characteristics are documented in the user's manual of Luna ODiSI-B [3]. The sensors have also been validated in [4], used in dynamic tests in [2], and used in FSI for the first time in [1].

We acknowledge that surface curvature may have introduced some variability in precise sensor positioning, particularly along the chordwise extent of the blade, where human error during installation is unavoidable. However, the same sensor layout was maintained consistently across all tests, ensuring that results are internally comparable. We have added a note on this to the revised manuscript, lines 312-318 section 3.2. "Blade strain response to unidirectional static point loading".

3. line 243: "...whereas the contribution of gravitational loads becomes negligible, potentially due to increased blade stiffening". This doesn't sound correct. Blade stiffening would be a valid hypothesis in case of bending moments. Here, the RBS sensor measures peak strain at $\theta = \pi$ or 0 which implies that axial stretching of the blades due to gravity is measured. In case of such an axial loading, blade stiffening cannot reduce the $\delta\varepsilon$ due to gravity. I think the reason for such an observation is different. In the blade frame, gravity acts along the chordwise and spanwise directions as a sinusoidal force whose frequency is determined by the rotational speed. In total, gravity imposes a $\sim$ 10 units of strain variation. But when the blade rotates faster, the system has less time to dynamically respond to a high-frequency forcing. Therefore, the gravity effect becomes invisible in the phase-averaged measurements beyond a certain rotation speed.

   We appreciate the reviewer's comment. The number of strain acquisitions per rotation, N^{ROT}, is never an integer value in our test cases. Therefore, when doing phase averaging across the bins of data we verified that the bins were not necessarily centred with the correct phase of the blade—there was data leakage between phase-averaged bins. The "stiffening" we had initially observed was then an artifact resulting from an error in data processing. We now changed figure 8 a) to show the temporal evolution of the spanwise averaged strain across the blade, for different rotating velocities, under a quiescent background. This figure clearly shows the increase of strain magnitude with the increase of the rotational velocity of the blades. Furthermore, no centrifugal stiffnening is observed, the fluctuations of strain across each cycle remain approximately constant ($\Delta\varepsilon = 10\ \mu\varepsilon$).

4. **Figure 9:** When comparing strain signatures across TSRs, changes in the effective structural response of the blade (including centrifugal pre-tension and any shift in modal properties) should be considered. At present, the role of blade structural dynamics is not discussed, despite being potentially important for interpreting off-design behavior.

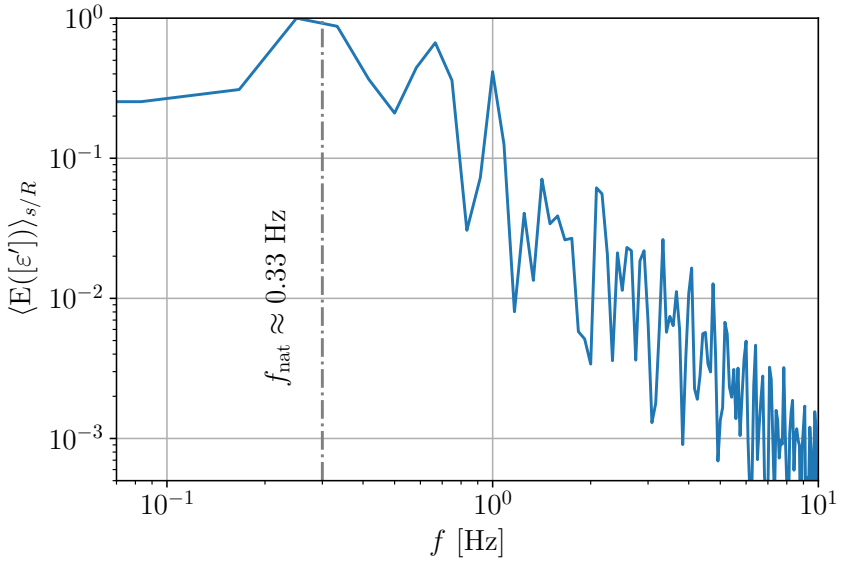

Figure 2: Spanwise ensemble average of the normalised PSD of the acquired strain fluctuations during free-decay test.

We agree that changes in the effective structural response of the blade—including centrifugal pre-tension effects and potential shifts in modal properties—could in principle influence the strain signatures observed across different λ. Figure 8 a) now partially addresses this point, as it shows that the $\Delta\varepsilon = 10$ $\mu\varepsilon$ remains constant across operating conditions - when considering the impact of gravity and centrifugal forces.

We performed a free-decay test on the blade to characterize the blade's fundamental natural frequency. These tests revealed a natural frequency of approximately 0.33 Hz (as you can see in figure 2 of the rebuttal), which is significantly lower than the blade passing frequencies ($St_\Omega = 3$) encountered in our experiments (ranging from approximately [3 Hz at lowest λ] to [18.25 Hz at largest λ], corresponding to the rotational frequencies tested). A note on this was added to the core text of the manuscript in section 3.2 "Blade strain response to unidirectional static point loading".

Given this separation, we do not expect resonance or significant dynamic amplification effects to compromise our measurements across the tested λ range. While centrifugal pre-tension does increase with rotational speed (scaling with Ω^2) and could potentially increase the natural frequency through geometric stiffening, the baseline natural frequency is sufficiently low that even a moderate increase would be unlikely to bring it into resonance with the operational frequencies. We expect the measured strain signatures therefore to reflect the approximated aerodynamic+centrifugal+gravitational forcing on the blade, with varying structural dynamics introduced by modal shifts of blade properties playing a minimal role in the frequency range of interest.

Moreover, we acknowledge that this is a relevant avenue to pursue for future work, that our experimental methodology can potentially resolve to help validating and cross-comparing numerical structural dynamics solvers.

5. **Figure 11:** It is difficult to draw strong conclusions from Figure 11 without comparing against an expected bending-moment/strain distribution under steady aerodynamic loading (e.g. BEM-based prediction). Such a reference could be used for normalizing the measurement data and render results from different sections comparable.

   We agree that comparing the measured spanwise strain distribution against BEM-based predictions would be highly valuable and represents an important future direction for this work.

   However, we consider such detailed modeling to be beyond the scope of the present paper, which focuses on the experimental characterization of FST effects on rotor blade loading. More importantly, it presents a proof of concept experimental technique to record blade dynamics during operation of the wind

turbine. The comparison you suggest-between high-fidelity measurements and BEM or other numerical predictions—is indeed an important next step and represents one of the key values of our experimental dataset.

To our knowledge, these measurements provide the first experimental data with sufficient spanwise resolution to enable meaningful validation of numerical algorithms (BEM, LES, actuator line methods, etc.) for predicting blade loads under turbulent inflow conditions. This validation exercise, while highly relevant, would constitute a substantial study in its own right, requiring:

- Detailed structural modeling of the 3D-printed blade geometry and material properties
- Comprehensive BEM simulations across all tested operating conditions and FST configurations
- Systematic comparison and uncertainty quantification

We believe this validation work would be best addressed in a dedicated follow-up study that can give proper attention to the modeling assumptions, uncertainty analysis, and interpretation of model-experiment comparisons.

We have now added to the revised manuscript section 3.2. "Blade strain response to unidirectional static point load", reflecting preliminary measurements conducted to assess the blade's response and strain signal to different and increasing loading scenarios to which the blade was exposed to in static conditions. We have now also added details on blade geometry and rotor design to Appendix C.

6. **line 357:** "The decreased rate of increase for $\lambda > \lambda_d$ reflects the aerodynamic stabilisation of the blade". I don't understand what this means. The decreased rate is most probably because of the reduced bending moment close to the blade tip, which behaves like a free end of a cantilever beam (see the previous comment).

   Here, by "aerodynamic stabilisation" we refer specifically to the reduction in lift-induced bending moments at above-design tip-speed ratios ($\lambda > \lambda_d$). At above-design λ, the effective angle of attack experienced by the blade sections decreases toward zero as the rotational velocity component increasingly dominates over the incoming wind velocity. This reduction in angle of attack leads to substantially decreased lift generation, and consequently lower bending moments acting on the blade. Moreover, under these conditions, the flow is also attached to the blade so the blade doesn't experience loads driven by aerodynamic unsteady events. The "decreased rate of increase" of Δ_s with λ reflects this aerodynamic effect-the blade experiences progressively less aerodynamic forcing as it operates further from its design condition. We understand that "aerodynamic stabilisation" is ambiguous, and decided to remove it from the manuscript. We have revised the text to clearly state that the reduced rate of increase reflects the decreasing lift forces and bending moments that result from operating at above-design λ, where the effective angles of attack are substantially reduced.

   Regarding your comment about the blade tip behaving as a free end: while the spanwise distribution of bending moments certainly influences the strain measurements (with expected reduction toward the tip), the observed trend with λ across all three spanwise locations suggests that the aerodynamic forcing mechanism-rather than purely structural effects-is the dominant factor in explaining the decreased growth rate of Δ_s as λ increases beyond λ_d.

   We have reviewed the wording of the paragraph in the revised version of the manuscript, and adjusted the discussion according to the above. This discussions sits now at the last paragraph of section 4. "Impact of λ and FST on turbine operation and time-averaged blade load".

7. **line 364:** "This suggests that at design conditions, the effects of FST on the time-averaged loads are mitigated by the operational conditions of the turbine." The observation that different FST levels have limited influence on time-averaged strain at design TSR is interesting and deserves deeper discussion. The current explanation is vague. I think, the authors should elaborate mechanistically.

   We appreciate the reviewer's comment. In fact, upon revisiting the analysis and including uncertainty, we observe that our initial argument was overstated, and have removed it from the revised manuscript.

Similarly to the last point, this discussions is now at the last paragraph of section 4. "Impact of λ and FST on turbine operation and time-averaged blade load".

8. **eq 11:** The proposed method for predicting FST-related RMS fluctuations assumes uncorrelated contributions. However, the manuscript also notes unsteadiness in rotational speed; in that case, strain fluctuations can be strongly correlated with speed variations and may not be separable by the proposed approach. Simultaneous analysis of rotation-speed fluctuations and strain (e.g. conditioning, coherence analysis, or decomposition techniques such as extended POD or conditional averaging) would be required to isolate the turbulence- driven component more convincingly. The possible influence of periodic forcing at blade-passing frequency (BPF) and its harmonics should also be addressed explicitly, and maybe eliminated priorly using notch filters.

   Thank you for this thoughtful comment regarding the decomposition method in what is now Equation 12 in the revised manuscript.

   While we do observe small variations in rotational speed ($\Delta\Omega \approx 9$rpm maximum at $\lambda = \lambda_d$), the frequency content of these motor-induced fluctuations is effectively decoupled from the blade dynamics due to the mechanical configuration. The motor is connected to the rotor through a 1:3 gear reduction. Moreover, the motor's controller frequency is set to a different frequency to it's operating velocity as it adjusts the action to correct drifts from rotational speed. We ensured that this was not affecting our measurements. The gear ratio combined with the mechanical damping inherent in the gear system ensures that high-frequency motor dynamics (of an order of magnitude larger) are significantly attenuated before reaching the blade. Consequently, the motor-induced speed variations and aerodynamic strain fluctuations occur in largely separated frequency bands, reducing concerns about strong correlation between these components.

   We now fully acknowledge in the revised manuscript (see section 3.3 "Blade loads in quiescent atmosphere") that even after subtracting the quiescent background measurements (RMS(ε'_{g+c})), a residual aerodynamic component remains in the quiescent background baseline. The blades generate lift even under quiescent inflow conditions, and this steady loading contributes to the measured strain. To correct this, the gravitational+centrifugal strain induced baseline would have to be taken in vacuum, and we were unable to find a sufficiently large vacuum chamber to test our turbine model, removing efficiently the residual aerodynamic component from the "wind-off" tests. Therefore, our estimate RMS(ε'_a) represents a first order and, the closest approximation to an aerodynamic-induced strain we can get with our current setup+experimental methodology.

   The sophisticated analysis methods you suggest (coherence analysis, extended POD, conditional averaging) would indeed provide a more rigorous separation of strain components. We are preparing new experiments and this is future work for a more fluid-structure interaction focused paper that we are working on. The current manuscript is already long and more general in focus across flow and blade dynamics.

   Regarding BPF and its harmonics, we now prove that these frequencies arise from wake forcing mechanisms interacting with the turbine blades and represent legitimate aerodynamic phenomena rather than artifacts to be filtered out. In the revised manuscript, we have added a new section (Section 7) exploiting concurrent blade strain and wake velocity measurements through cross-power spectral density (CPSD) analysis. The CPSDs reveal the spectra of the cross-correlation function between wake and blade measurements, confirming the presence of the same three dominant frequencies ($St_\Omega \in \{1, 2, 3\}$) observed in the PSDs (Section 6). This demonstrates the relevance of these dynamics to the coupled wake-blade system and shows which flow regions and frequencies contribute most to blade loading. We note that CPSDs quantify correlation but do not establish causality. Moreover, the fact that the PSDs of the strain dynamics at "wind-off" conditions present negligible energy at $St_\Omega = 3$ (presented in the revised manuscript in figure 9), which emerges under "wind-on" conditions highlights, by process of elimination, the presence of flow-driven mechanisms generated at the tip of the blade and propagating into the wake that interact with the blade of the turbine. We now explore the aerodynamic nature of this dynamic in the last paragraph of section 6.1. "Integrated Spectral Energy Across Frequencies".

9. **line 382:** "TIP consistently exhibits the largest fluctuation levels across all operating conditions and FST cases." The statement that the tip consistently exhibits the largest fluctuation levels may be expected simply because the tangential velocity (and therefore sensitivity to rotation- rate variability) increases with radius. Normalization choices and sensitivity to RPM variations should be discussed before interpreting this result as purely aerodynamic.

   You are correct that higher tangential velocity at the tip amplifies sensitivity to both aerodynamic forcing and rotational speed variations. However, this is precisely the effect we aim to characterize, understanding how FST and operation-induced strain fluctuations scale across the blade span under realistic operating conditions, including the natural amplification at outboard sections. The sensitivity to RPM variations is on its own an aerodynamic effect. As the blade rotates faster, it experiences an increased relative incoming velocity U_{rel} (to the airfoil profile) and therefore, remains of interest to assess. While normalisation by local dynamic pressure could isolate relative aerodynamic sensitivity, the approximation of the aerodynamic strain at the tip is of primary interest for structural integrity assessment and represent the actual strain experienced by the blade during operation. We have added discussion on the impact of normalising $\text{RMS}(\varepsilon'_a)$ by U^2_{rel} in the paragraph starting in line 494 of the revised manuscript.

10. **line 385:** "...a marked increase in overall strain fluctuations at $\lambda \approx 3.5$ is observed, potentially emphasizing the influence of the unstable regime of partially stalled to partially attached flow conditions" I don't think there is enough evidence not enough to support this partial stall hypothesis. I find it more probable that there's a structural natural frequency of the blade close to the frequency associated with that rotational speed.

    We respectfully disagree with the structural resonance hypothesis for several reasons. First, as mentioned in our response to comment 4, free-decay testing of the blade revealed a fundamental natural frequency of approximately 0.33 Hz, which is significantly lower than the rotational frequencies encountered across all tested operating conditions. Second, the aerodynamic interpretation is consistent with established wind turbine literature: operation below the design λ is characterized by elevated angles of attack that can lead to intermittent flow separation and reattachment, creating a bistable operating condition. The marked increase in strain fluctuations at $\lambda \approx 3.5$ is consistent with this aerodynamic mechanism.

    We acknowledge that definitively proving the partial stall hypothesis would require flow visualization or surface pressure measurements to directly observe the flow separation patterns. However, given the confirmed separation between structural natural frequencies and operating frequencies, combined with the well-documented aerodynamic instabilities at sub-optimal λ conditions, we believe the aerodynamic interpretation is the most plausible explanation.

11. **line 398:** "Moreover, at $\lambda \geq \lambda_d$, conditions in which the flow is attached to the blade, increased TI consistently increases $\text{RMS}(\varepsilon'_a)$ across the three sections of the blade". Figure 12 doesn't support this observation.

    At fixed λ above $\lambda > \lambda_d$, $\text{RMS}(\varepsilon'_a)$ generally increases with the increase of FST TI. However, we agree that this is not consistent across cases, especially between FST "flavours" B and C. We have then decided to remove the statement from the revised manuscript.

12. **line 403:** "These results suggest that, from an aerodynamic-induced fatigue damage perspective, it is preferable to maintain wind turbines operating at slightly above design conditions with the compromise of the increased contribution of centrifugal loads, rather than slightly-below design." The conclusion recommending operation slightly above design TSR from a fatigue perspective appears too general. If the observed RMS behavior is influenced by the blade's structural response and/or resonance proximity, it may not generalize across turbine designs.

    The added discussion upon visiting the reviewer's comments clarifies the non-proximity of the blade's structural response and resonance to the operating conditions - see the answers to points no. 4 and 8 for instance. However, we acknowledge that our initial argument was an overstatement and that our blade is not representative of real-life turbine structures - for instance, our blade is monolithic and doesn't have

an internal structure as real-life wind turbines posess. Therefore, we have removed the original statement from the revised-manuscript text.

13. **line 428:** "The PDFs under quiescent background conditions follow a Gaussian-like profile consistent with the periodic impact of the combined centrifugal+gravitational loads acting on the blades."Periodicity alone does not imply a Gaussian distribution; a purely periodic signal sampled uniformly in phase typically yields a non-Gaussian PDF. The authors should clarify the processing used and the basis for expecting Gaussian statistics.

    Thank you for this important clarification. You are correct that periodicity alone does not imply a Gaussian distribution—a purely periodic signal would indeed produce a non-Gaussian PDF.

    The observed Gaussian-like profile in the quiescent background conditions results from the spatial aggregation method used to construct the PDFs in the original Figure 14. The strain data was aggregated across a spanwise region of the blade, combining measurements from multiple sensor locations. Our power spectral density analysis demonstrates that the strain components at different spanwise locations, are exposed to different dynamics - for instance, the chordwise component is not subjected to $St_\Omega \in \{1, 2, 3\}$ dynamics as observed in figure 21 of the revised manuscript. When aggregating these spatially distributed, weakly correlated signals, the Central Limit Theorem applies: the sum of multiple uncorrelated or weakly correlated random variables tends toward a Gaussian distribution, even if the individual signals are not themselves Gaussian.

    In response to your comment, we have completely revised this section of the manuscript to include additional analysis showing PDFs of individual strain components (chordwise and spanwise) at specific blade locations (now Figure 18). We have also adapted the analysis accordingly—see lines 531:554 of the revised manuscript. This decomposed analysis reveals that the spanwise component under quiescent conditions exhibits the expected non-Gaussian PDF associated with purely periodic loading from combined centrifugal and gravitational effects especially observed at the root and low λ, while the chordwise component shows different behavior due to its distinct loading mechanisms. We believe this additional analysis strengthens the interpretation and addresses your concern comprehensively.

14. **line 459:** "The profiles of $E(\varepsilon'_a)$ are estimated from $E(\varepsilon' - E(\varepsilon'_{g+c}))$." Once again, such a decomposition does not necessarily isolate aerodynamic loading if the components are correlated or if periodic contributions remain. This may explain why the spectra remain dominated by BPF in Figure 17. A more robust separation approach should be discussed.

    We now acknowledge in the revised manuscript that our decomposition represents a first-order approximation rather than complete isolation of aerodynamic effects. However, the persistence of BPF peaks in $E(\varepsilon'_a)$ does not indicate failure of our separation methodology-these reflect genuine periodic aerodynamic forcing inherent to rotor operation.

    The key evidence supporting our approach is shown in figure 3 of the rebuttal document, presenting the strain spectra of the blade under quiescent background conditions. Under quiescent conditions at $\lambda = 4$, the strain spectra show no peak at $St_\Omega = 3$, yet this peak emerges prominently under "wind-on" conditions, demonstrating it arises from aerodynamic effects rather than from incomplete removal of gravitational/centrifugal effects.

    While more sophisticated techniques (coherence analysis, conditional averaging, POD) could provide better separation of correlated components, the clear emergence of the $St_\Omega = 3$ peak only under "wind-on" conditions at $\lambda = 4$ validates that our simple subtraction effectively reveals the additional aerodynamic forcing mechanisms introduced by FST, which is the primary objective of this analysis. To note the increase in energy at $St_\Omega \in \{3, 4\}$ for $\lambda = 6.5$ due to an increased relative velocity to the blade in line with the increased rotational velocity as these tests were not run in a vacuum chamber. This discussion has been added to the manuscript, in sections 3.2. "Blade strain under gravitational and centrifugal loading" and section 6.1 "Integrated Spectral Energy Across Frequencies".

15. **line 514:** "...ε'_a and ε'_g are uncorrelated." This comment implies that the authors disregard the results

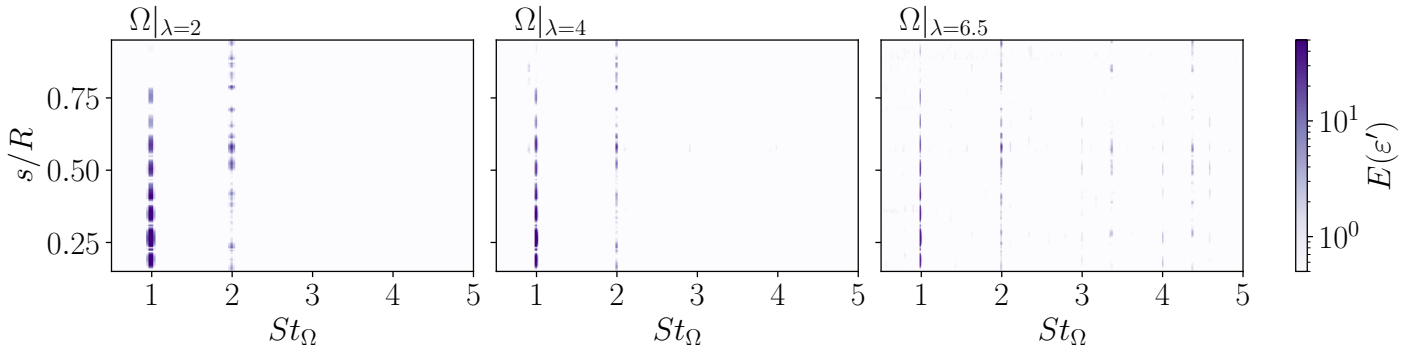

Figure 3: Power-spectral density of the fluctuating strain's response at selected $\Omega|_\lambda$ under quiescent background conditions.

shown in figure 17. Since both components can contain rotor-synchronous periodicity, the correlation assumption should be revisited.

We appreciate the reviewer's observation and acknowledge that our statement requires clarification. Our assumption is not that ε'_a and ε'_{g+c} are globally uncorrelated, but that the forcing mechanisms driving these components are decorrelated (see now line 664 of the revised manuscript). While both produce periodic forcing at BPF and harmonics, they arise from fundamentally different physical mechanisms: gravitational/centrifugal effects stem from inertial forces in the rotating frame, whereas the aerodynamic rotor-synchronous forcing originates from coupled wake interactions as evidenced in our CPSD analysis (Section 7). By subtracting $E(\varepsilon'_{g+c})$ measured under identical rotational conditions, we remove the inertial contribution while preserving the aerodynamic rotor-synchronous content. The key empirical validation is that certain spectral features (e.g., the $St_\Omega = 3$ peak at $\lambda = 4$) emerge only under "wind-on" conditions, and are absent in quiescent baselines (see figure 3 of the rebuttal), confirming that our decomposition successfully separates these mechanistically distinct sources of rotor-synchronous excitation. We have revised the text to clearly state that our assumption is the decorrelation of the forcing mechanisms rather than the resulting strain responses. Once more, this discussion has been added to the manuscript, in sections 3.2. "Blade strain under gravitational and centrifugal loading" and section 6.1 "Integrated Spectral Energy Across Frequencies".

Minor comments:

1. **line 308:** "...and edgewise ε_a^f..." should be ε_a^e I guess.

   This has been fixed in the reviewed version of the manuscript. Please note the change in notation for the benefit of clarity, where "flapwise" with the subscript f has been changed to spanwise, with a subscript s. Similarly, edgewise with subscript e has been changed to chordwise, with subscript c.

2. **line 421:** "Figure 15 represents..." I guess, it should be Figure 14.

   This has been fixed in the reviewed version of the manuscript. Please note the change in figures referencing and the referenced line is now line 531.

References

[1] F. J. G. de Oliveira, Z. S. Khodaei, and O. R. H. Buxton. Simultaneous measurement of the distributed longitudinal strain and velocity field for a cantilevered cylinder exposed to turbulent cross flow. *Experiments in Fluids*, 65(9):134, 2024.

[2] Y. Li and Z. Sharif-Khodaei. Shape sensing of composite shell using distributed fibre optic sensing. *International Journal of Mechanical Sciences*, 286:109859, 2025.

[3] Luna Inc. ODiSI-B optical distributed sensor interrogator data sheet. `https://lunainc.com/sites/default/files/assets/files/data-sheet/Luna%20ODiSI%206000%20Data%20Sheet.pdf`, 2022.

[4] C. Xu and Z. S. Khodaei. Shape sensing with rayleigh backscattering fibre optic sensor. *Sensors*, 20(14):4040, 2020.